Nonlinear Gulf Stream Interaction with Deep Currents: A Numerical Simulation

David E. Dietrich [*,1], Avichal Mehra [2], Robert L. Haney [3], Malcolm J. Bowman [4], and Yu-Heng Tseng [1]

Abstract

A two-way-coupled duo grid primitive-equations-based ocean model is used in a 75-year simulation of the North Atlantic Ocean, Caribbean Sea and Gulf of Mexico region between 10° N and 73° N. All advection and horizontal pressure gradient terms are fourth-order accurate on a semi-Collocated control volume grid. By construction of surface freshwater and heat fluxes, the model multi-year *ensemble mean annual cycle* surface layer temperature and salinity converge to the climatological cycle. Hellerman annual cycle wind forcing is used. The duo grid resolutions are: 1/2° east of 60° W; 1/6° west of 60° W; 30 z-levels. Upwind-based fluxes across 60° W give nearly seamless grid coupling. Open boundary conditions derived from a one degree resolution global model are applied at 10° N. Model results show: total Gulf Stream (**GS**) separation at Cape Hatteras (**CH**) as observed, and a mean separated GS path close to the observed mean path. The model Deep Current System (**DCS**: the shelf slope and deep western boundary current) strongly affects the GS separation and path. Only after ~ 10 years of simulation, when the Labrador-Sea-modified dense DCS water arrives in the Grand Banks shelfbreak area, does the GS separation and path come into close agreement with observations. The wedge shaped region between the separated Gulf Stream and continental shelf slope is filled with eddies, including intense warm cores that pinch off the northern tips of Gulf Stream meanders. The isopycnal surfaces have a strikingly small slope in this region's interior in both Yashayaev's climatology (2002) and time mean model results, indicating eddy dynamics characteristic of baroclinic instability rather than diffusive lateral mixing between the GS and DCS.

Key words: Deep currents, Western boundary currents, Oceanic eddies, Modelling

1 Introduction

Gulf Stream (GS) separation near its observed Cape Hatteras (CH) separation location, and its ensuing path and dynamics, is a challenging ocean modeling problem. If a model GS separates much farther north than CH, then northern GS meanders that pinch off warm core eddies (rings) are not possible or are strongly constrained by the Grand Banks shelfbreak. Cold core rings pinch off the southern GS meanders. The rings are often re-absorbed by the GS.

These important warm core rings enhance heat exchange and, especially, affect the northern GS branch after GS bifurcation near the New England Seamount Chain. This northern branch gains heat by contact with the southern branch water upstream of bifurcation, and warms the Arctic Ocean and northern seas, thus playing a major role in ice dynamics, thermohaline circulation and possible global climate warming. These rings transport heat northward in the wedge shaped region between the separated GS and the DCS. This region has nearly level time mean isopycnals. The eddy heat transport convergence/divergence enhances the shelfbreak and GS front and thus also increases watermass transformation. The fronts are maintained by warm advection by Florida Current and cold advection by the DCS. Thus, the GS interaction with the DCS through the intermediate eddy field is climatologically important.

The DCS path affects gasification of ice-like methane hydrates stored on the ocean bottom, below depths where methane freezes ($\sim 4°C$, depending also on pressure-depth). It is thought that this methane, after gasifying and escaping into the atmosphere, may oxidize and add huge amounts of $CO2$ (Katz et al., 1999), a greenhouse gas that, unlike the water vapor byproduct, does not precipitate out, thus contributing to global warming. As suggested by Lai (2003), strongly exothermic biogeochemical processes occurring within the methane gas bubbles generated in the ocean depths (Kennett et al., 2000) may: significantly warm the DCS; lead to positive feedback, including DCS recirculation in the northern seas and Arctic Ocean; and further affect thermohaline circulation by annual cycle ice melting/freezing (that have strong stratification effects and resulting air-sea heat exchange effects) in the Arctic Ocean and northern seas. Vertical mixing of the warm water is capped by overlying warmer water until the warm water spreads and flows to the high latitude ocean where it

* Corresponding Author
[1] Center for Turbulence Research, Stanford University, Stanford , CA 94305-3035
[2] GeoResouces Institute, Mississippi State University, Bldg. 1103, Rm. 233, Stennis Space Center, MS 39529-6000
[3] Department of Meteorology, Naval Postgraduate School, 589 Dyer Road, Room 254, Monterey, CA 93943-5114, USA
[4] Marine Sciences Research Center, State University of New York at Stony Brook, Stony Brook, NY 11794-5000, USA

melts sea-ice and enhances coastal polynia. This generates saltier deep water possibly leading to methane hydrate suspension and rising to warmer levels, where it gasifies and increases the biogeochemical warming. Significantly, methane hydrates contain more fossil fuel energy than in coal and oil combined, enough to melt as much as a 150% of the sea-ice in the world ocean, depending on biogeochemistry deatils. These processes are coupled to the GS path and dynamics. As further noted by Lai (2003), this possibility warrants careful study, especially in view of observed recent global warming (IPCC, 2001) and oxygen depletion (Joos et al., 2003) in the ocean depths near the methane hydrate levels. A major concern is that anthropogenic perturbation of the system may lead to even stronger rapid warming than the $\sim 10^{\circ}C$ Arctic atmospheric temperature rise that occurred in 10-20 years at the end of the last glacial maximum (Rossby and Nilsson, 2003).

Thus, modeling the thin narrow dense DCS material is critical. It is also a unique modeling challenge due to its small scale and long $O(1-10$ years) material travel time from its northern source regions to the shelfbreak region between Cape Hatteras and the Grand Banks where it interacts strongly with GS separation and path. In order for the DCS to reach the latter region with sufficient intensity to properly affect GS separation and path, it must not be overly diluted by numerical dissipation and dispersion. The DieCAST model, used herein to study this and related effects, is robust using very small dissipation and low dispersion fourth-order accurate numerics (Dietrich, 1997). The importance of these features is clearly demonstrated by a companion dissipation sensitivity study (Dietrich et al., 2004a).

DieCAST's ability to simulate wakes and recirculations (closely related to GS separation physics) has been shown in comparison with laboratory experiments of $2-D$ Von Karman wake vortices (Dietrich et al., 1996); that study also showed significant stratification effects in simulated wake vortices from a $3-D$ island patterned after Barbados. DieCAST applicability to ocean boundary current separation has also been validated by a variety of observations in: the Black Sea, whose coastal region is dominated by energetic recirculation eddies in the wakes of coastal abutments in a strongly stratified environment having major annual cycle effects (Staneva et al., 2001); in the Gulf of Mexico (Dietrich et al., 1997); Mediterranean Sea (Fernandez et al., 2003); and Adriatic Sea (Cushman-Roisin et al., 2003).

Besides GS separation and mean path, realistic simulation of GS natural variability is also important. GS separation occurs when the shelfbreak current from the Florida Straits angles toward deeper water. If it does not separate at CH, the observed separation location, but separates much later as is common in North Atlantic Ocean models, it then remains too close to the shelfbreak to allow northward (shoreward) meanders to develop freely and pinch off warm core eddies (rings). The distance from the mean GS current to the shelfbreak

must be at least comparable to the Rossby radius of deformation for this to happen. The highly energetic, nonlinear turbulent GS system provides a significant amount of geophysical "noise" to the climate system. Such "noise" may affect climate through fundamentally nonlinear stochastic resonance (Velez-Belchi et al., 2001); such resonance may be associated with nonlinear effects of changes relating to freshwater sources and sinks (Rossby and Nilsson, 2003), changes of North Atlantic Deep Water formation (Rahmstorf and Alley, 2002) and nonlinear GS interaction with the DCS seen in results of the present study. Such variability occurs naturally in the ocean by itself; for example, even with annual cycle forcing, constructed using observed annual cycle surface wind, heat flux and freshwater source/sink conditions, there is significant interannual variability in Mediterranean Sea model simulations (Fernandez et al., 2003). Another example of particularly strong natural interannual variability is the Gulf of Mexico (Dietrich et al., 1997), which is dominated by the Loop Current and its irregular major eddy shedding, independent of annual cycle forcing, having a mean time-scale of ~ 270 days.

Two recent major North Atlantic Basin model comparison studies are: DYNAMO (1997) and DAMEE-NAB (2000). None of the DYNAMO models at $1/3^\circ$ horizontal resolution was able to simulate the observed GS separation at CH. This failure using only moderate horizontal resolution was not unexpected, because of the importance of fine-scale vorticity dynamics and bathymetry near CH (Dengg at al., 1996). Coastal abutments such as CH often lead to boundary current separation; examples are ubiquitous in nature, a prime example being the Black Sea whose coastal circulation is dominated by recirculation eddies in the wakes of coastal abutments (Staneva et al., 2001). Besides isobath curvature near the CH abutment, the upstream convergence of isobaths also plays an important role in GS separation (Stern, 1998).

In the DAMEE model intercomparison experiment using HR (Hellerman and Rosenstein, 1983) climatological wind forcing, all but one of the models failed to simulate GS separation at CH. The exception was ROMS (Haidvogel et al., 2000), which got GS separation at the proper location without resolving the major CH coastal abutment. Hurlburt and Hogan (2000) report that when sufficient resolution is used to address nonlinear GS separation dynamics at CH using the NLOM model (Hurlburt and Thompson, 1980), realistic GS separation and other inherently nonlinear features are well simulated using HR winds, *even though* the linear version of the same model shows unrealistic wind-stress-curl-induced GS separation for 11 different wind stress climatologies including HR winds (Townsend et al., 2000); the linear effects of wind stress curl do not explain the observed GS separation and path, but instead give two paths, both very different from the observed one. Thus, the ROMS low resolution GS separation at CH is surprising.

The DieCAST ocean model adaptation for the present North Atlantic study is described in Section 2. In Section 3, the modeled North Atlantic general circulation is compared with observations, focusing on the GS and DCS; results before and after DCS establishment show dramatic effects of the DCS on GS separation and path, reinforcing findings by Dietrich et al. (2004a). Further mechanisms relating to GS separation are discussed in Section 4. Future work is suggested in Section 5. Concluding remarks are given in Section 6.

2 Model and Experiment Design

We use the z-level DieCAST ocean model adapted to the North Atlantic Ocean/Caribbean Sea/Gulf of Mexico system.

The model uses:

a) fourth-order accurate numerical approximations for all terms, except a conventional second-order accurate hydrostatic vertical pressure gradient, in a semi-collocated control volume framework (Sanderson and Brassington, 1998);

b) an incompressibility algorithm having low numerical dispersion associated with its required interpolations (Dietrich, 1997)

The semi-collocated grid avoids the large numerical dispersion resulting from evaluating the large Coriolis term on the conventional staggered Arakawa "c" grid. Fourth-order accurate advection further reduces numerical dispersion. Thus, the model is formally accurate. It is also robust using very low total (explicit plus numerical) dissipation.

The model domain covers the North Atlantic basin from 10° N to 73° N and from 97.5° W to 0° W. To reduce the computation required, a duo grid approach is used; the grids are coupled using upwind-based boundary flux approximations as used by Dietrich and Mehra (1998) for the Santa Barbara Channel nested in the California Current system. The western North Atlantic, Gulf of Mexico and Caribbean Sea require high resolution to resolve the GS separation region and critical narrow straits. West of 60° W, 1/6° resolution is used; east of 60° W, 1/2° resolution is used. The grids are fully two-way coupled each time step, with one coarse grid cell overlap (3×3 fine grid cells). The results are virtually seamless at the duo grid interface (Dietrich, 2002). There are 30 model layers, geometrically expanding from 41.6 m thick at the top to 738 m thick at the bottom (maximum depth 5000 m). Open southern boundary conditions are derived from a one degree global implementation of the DieCAST ocean model.

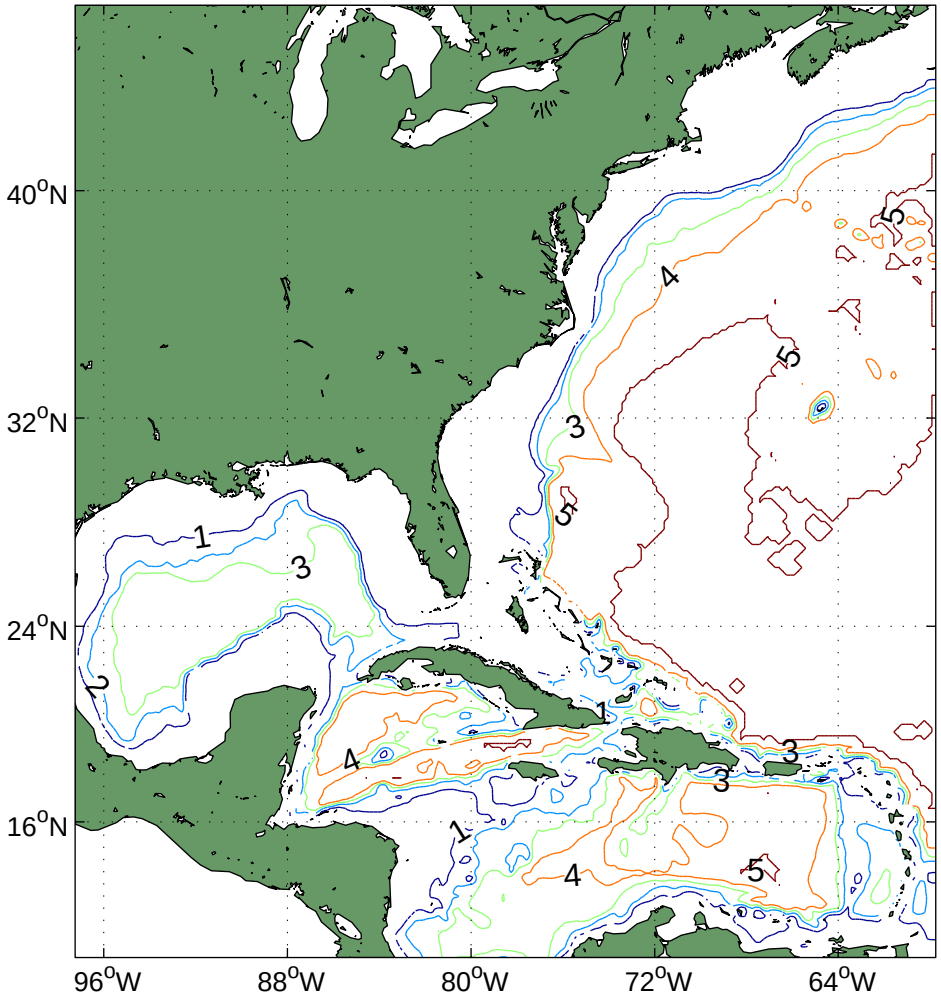

Fig. 1. Western (1/6° resolution fine grid) domain bathymetry (depths are in km).

Figure 1 shows the higher resolution western domain bathymetry; Figure 2 shows the lower resolution eastern domain. The map scale factors are different in these two plots. To avoid potentially disastrous unphysical vortex stretching in the northeast corner of the eastern domain, the real bathymetry is replaced by a shelfbreak patterned after the shortcircuited Arctic Ocean, rather than using a conventional vertical wall approach.

To resolve the critical Caribbean Sea passages and reduce computation, the duo grid interface is placed just east of the Caribbean Sea passages, and the western fringe of the Labrador Sea (north of 45° N and west of 60° W) is excluded and an idealized shelfbreak is used along 60° W in the eastern domain (Figure 2), again to minimize unrealistic vortex stretching.

Surface boundary conditions are derived from monthly climatology. The wind forcing is by monthly average HR climatological winds.

Heat and freshwater fluxes at the sea surface are computed such that the model

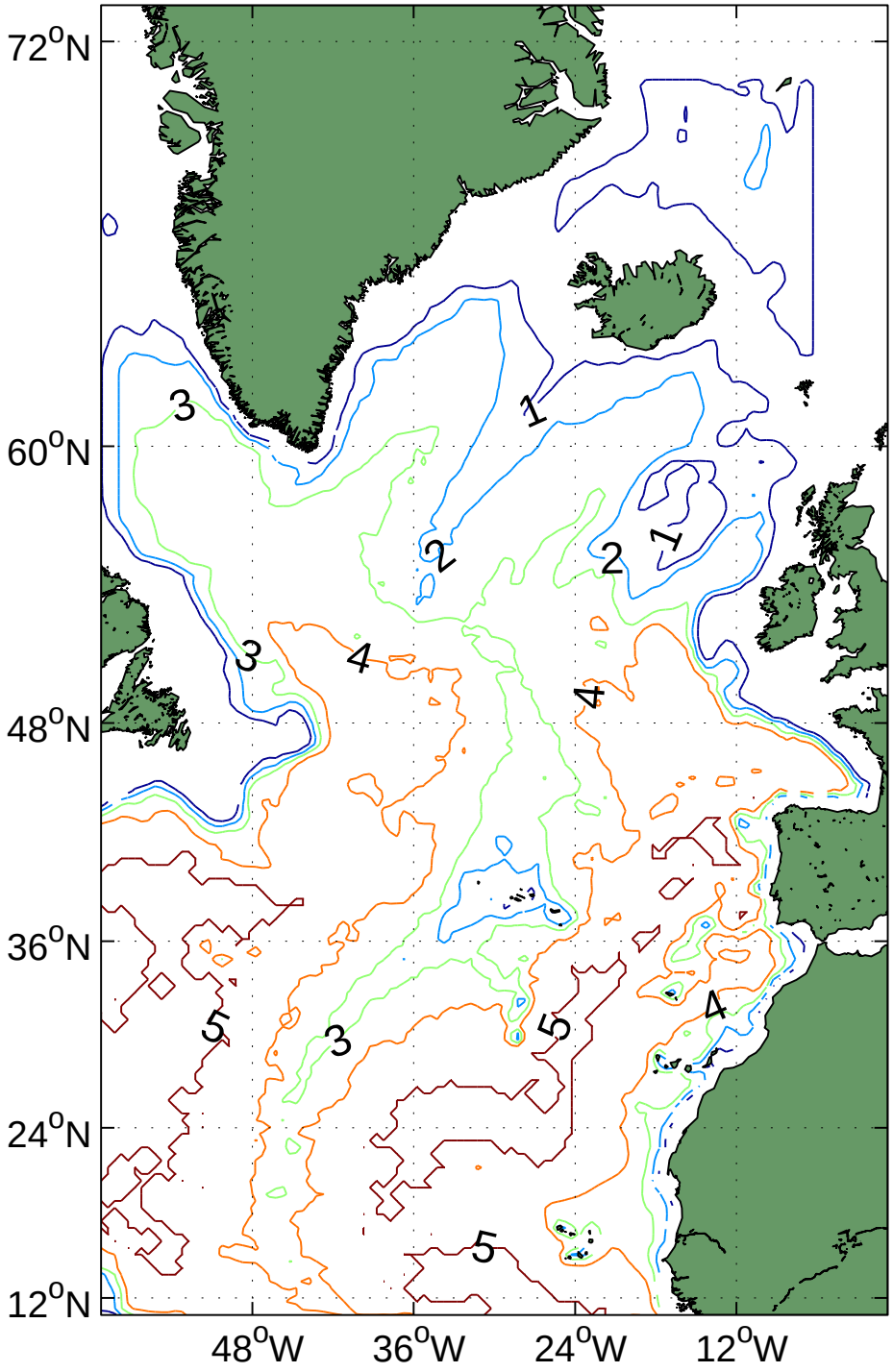

Fig. 2. Eastern (1/2° deg resolution coarse grid) domain bathymetry (depths are in km) showing shelfbreak bathymetry in the shortcircuited Arctic Ocean and western Labrador Sea.

multi-year mean annual cycle of surface temperature and salinity follow the observed climatological annual cycle (Dietrich et al., 2004b). This new surface buoyancy flux condition avoids problems (reduced annual cycle amplitudes and phase lags, and excessive damping of surface fronts) attributed to conventional restoring (Killworth et al., 2000).

Levitus climatology is used for initial conditions and for surface thermohaline forcing until model year 13, when it is replaced by an improved (less smoothed) surface climatology (Yashayaev, 2002). The annual mean surface temperature in the GS region from Yashayaev climatology (Figure 3) is consistent with the observed GS separation near CH.

Below-surface-layer model temperature is restored toward climatology in a buffer zone 20 gridpoints wide along open northern lateral boundaries. Salinity is not restored, because that does not conserve salt material and has no physical basis. Instead, a 0.2 Sv inflow of freshwater is spread uniformly along the open northern boundary to parameterize Arctic Ocean net river inflow (Bacon et al., 2002) and a 0.018 Sv Gulf of St. Lawrence freshwater volume source is also specified (Chapman and Beardsley, 1989).

All *externally* specified mass inflows (freshwater) are in the eastern, coarse grid domain; these are added to the inflow from the fine grid western domain and to the integrated e-p (evaporation - precipitation, derived as indicated by Dietrich et al. (2004b) to get a net eastern domain inflow; then, this net inflow is subtracted uniformly at the southern boundary ($\sim$ 0.02 Sv as it turns out) to be consistent with incompressibility. An alternate approach, not used herein, is to apply this volume correction at the surface (e.g., in a global model having closed lateral boundaries), using the mean diffusivity between the top two layers to maintain observed climatological annual cycle surface layer salinity. This approach is consistent with the long term climatological state (near zero mean sea level change) and with the rigid-lid approximation used in this model, in which there can be no mean surface height change. Thus, the rigid lid is slightly porous; the divergence of the barotropic mode (vertically integrated horizontal velocity) is very small but not exactly zero.

Based on the $\sim$ 100 km scale of the CH abutment, the constant $10m^2/s$ eddy viscosity used in the western domain, and the GS velocity ($\sim 1m/sec$), the Reynolds number is $O(10,000)$ for the primary GS separation scale. The Rossby number for these scales is $O(0.1)$. Both domains use near-molecular background vertical viscosity and diffusivity, with modified Pacanowski and Philander Richardson-number-based mixing as described by Staneva et al. (2001). Thus, the inertia terms are strong in the CH region, as necessary (but not sufficient, as a robust DCS is also required as will be shown herein) for nonlinear inertial separation.

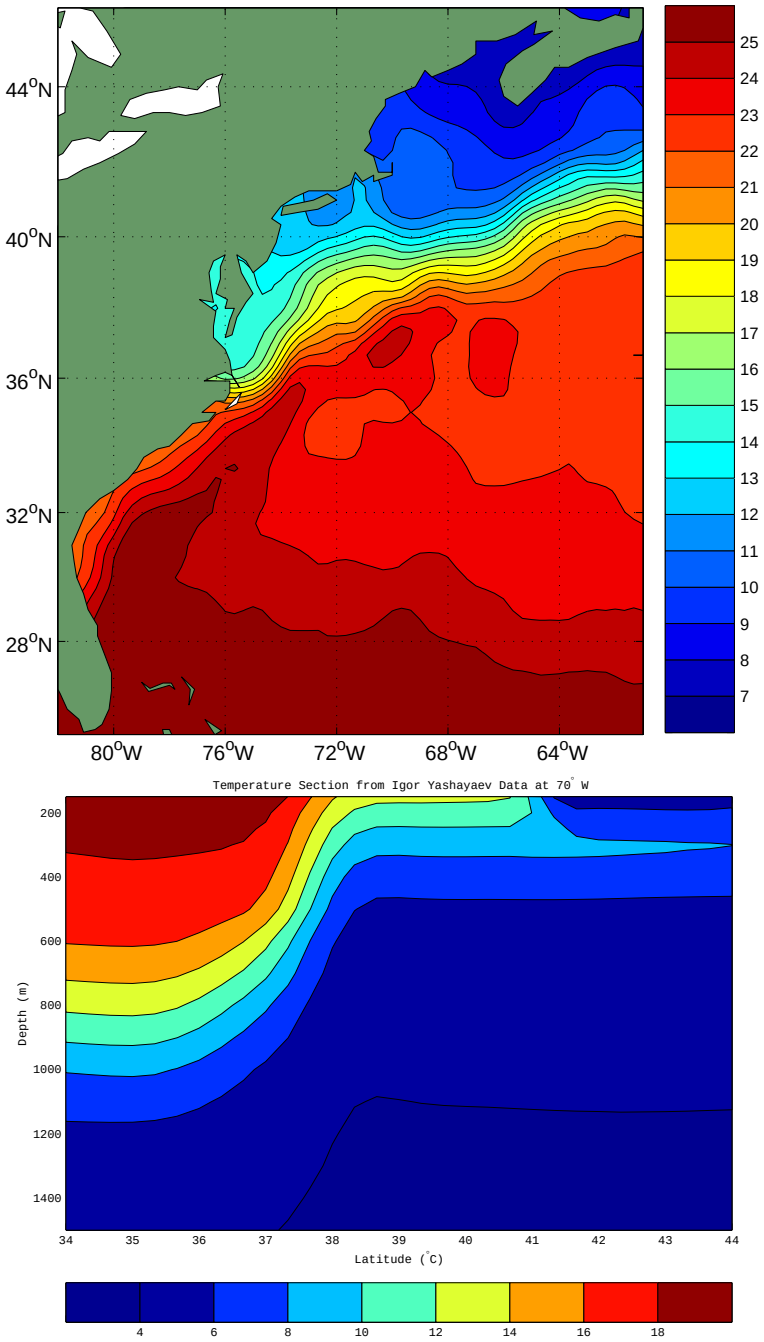

Fig. 3. Surface layer annual mean Yashayaev temperature ($^{\circ}C$) climatology in the western domain GS region (west of 60° W) of the duo grid DieCAST north Atlantic model(top panel); Vertical/latitudinal cross-section of annual mean Yashayaev potential temperature ($^{\circ}C$) climatology at 70° W, showing highly nonlinear, non-diffusive flattening of isopycnals between Gulf Stream and Grand Banks (bottom panel)

This overall model setup is the same as that used by Dietrich et al. (2004a) except: the truncated Labrador Sea shelfbreak is wider in the present case, which reduces DCS; the hydrostatic vertical pressure gradient is second-order-accurate rather than fourth-order-accurate; and a single 75-year run is made to show long term behavior in the present case rather than the shorter runs used to explore dissipation effects in Dietrich et al. (2004a).

We now briefly discuss the model's robustness with very low dissipation (large cell Reynolds number), which is a major advantage in view of the ocean's nearly inviscid nature. Scaling estimates of individual advection components can underestimate the effective advection time scales and overestimate their local impact, when their sum nearly cancels. If the advection components cancel exactly (e.g., as is approximately true by definition for a quasi-steady, high Reynolds number barotropic mode flow component), first- and third-order-accurate upwind methods are relatively inaccurate (rigorously) compared to centered second- and fourth- order-accurate methods, respectively; if they cancel approximately, as they tend to in nature due to the quasi-steady nature of the important slow mode dominant forcings, upwind methods are still relatively inaccurate. Thus, the cell Reynolds number limit of $O(1)$, which is roughly equivalent to first order accurate upwind advection in the absence of explicit diffusion, is only a rough guideline, rather than a rigorous requirement to avoid unphysical numerical overshoots (Roache, 1998). Fourth-order-accurate advection allows one to push well beyond this already soft cell Reynolds number limit, while avoiding large overshoots common to second-order-accurate centered methods (Dietrich, 1997), as clearly demonstrated by the present results. The duo grid model runs at ~ 200 model days per day of computer time on a PC using a single 2.0 gigahertz P4.

3 Results

3.1 Before and After DCS Interaction with GS Separation

The transient GS behavior during the first five model years is strikingly different from the long term behavior (Figures 4 - 6).

During the first model year (not shown), bathymetry-induced strong inertial dynamics lead to early partial GS separation near CH. However, the separated portion of the model GS moves northward to the Grand Banks shelfbreak during the next few model years. It then moves back southward to the observed CH separation point and mean downstream path after ~ 10 model years, and remains close to the mean observed path throughout years $10-75$ (end of the present simulation).

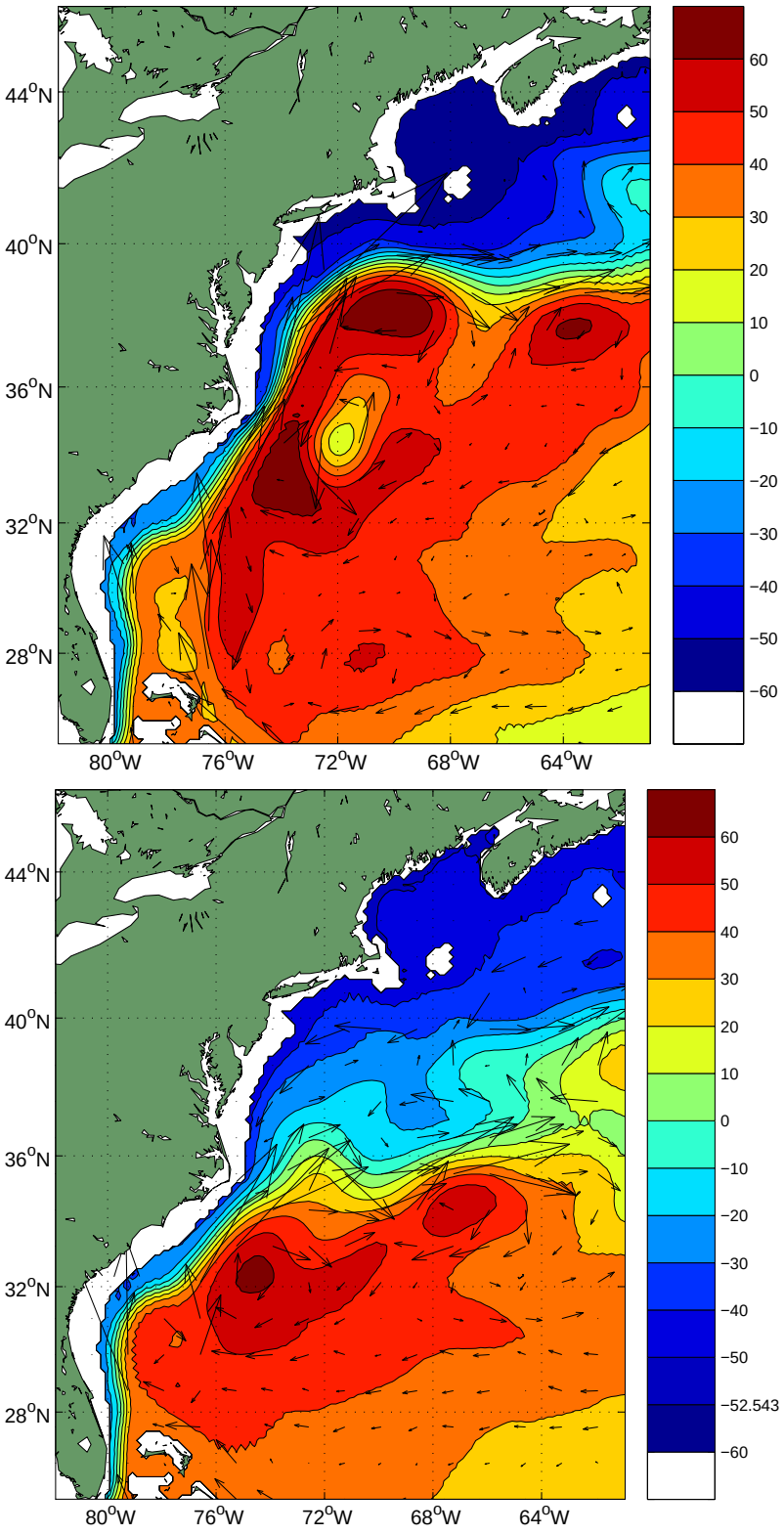

Fig. 4. Time mean sea surface height (cm) and 700 m depth velocity vectors in the 1/6 degree resolution western domain during years $0-5$ (top) and during years $66-75$ (bottom). The maximum velocity is 78 cm/s (top) and 38 cm/s (bottom).

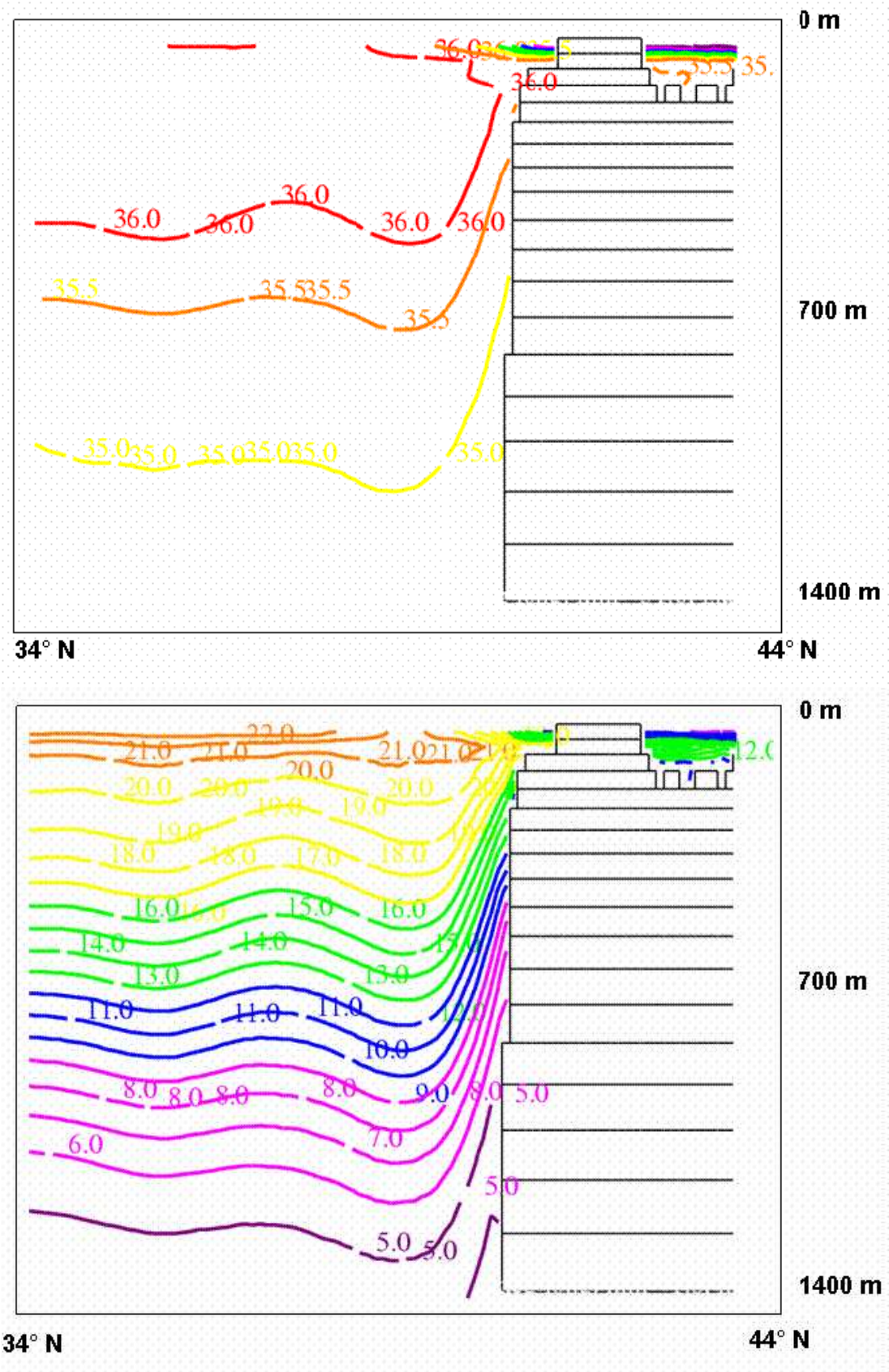

Fig. 5. Vertical/latitudinal cross-sections at 70° W of time-averaged salinity (top) and temperature (bottom) during years 0-5.

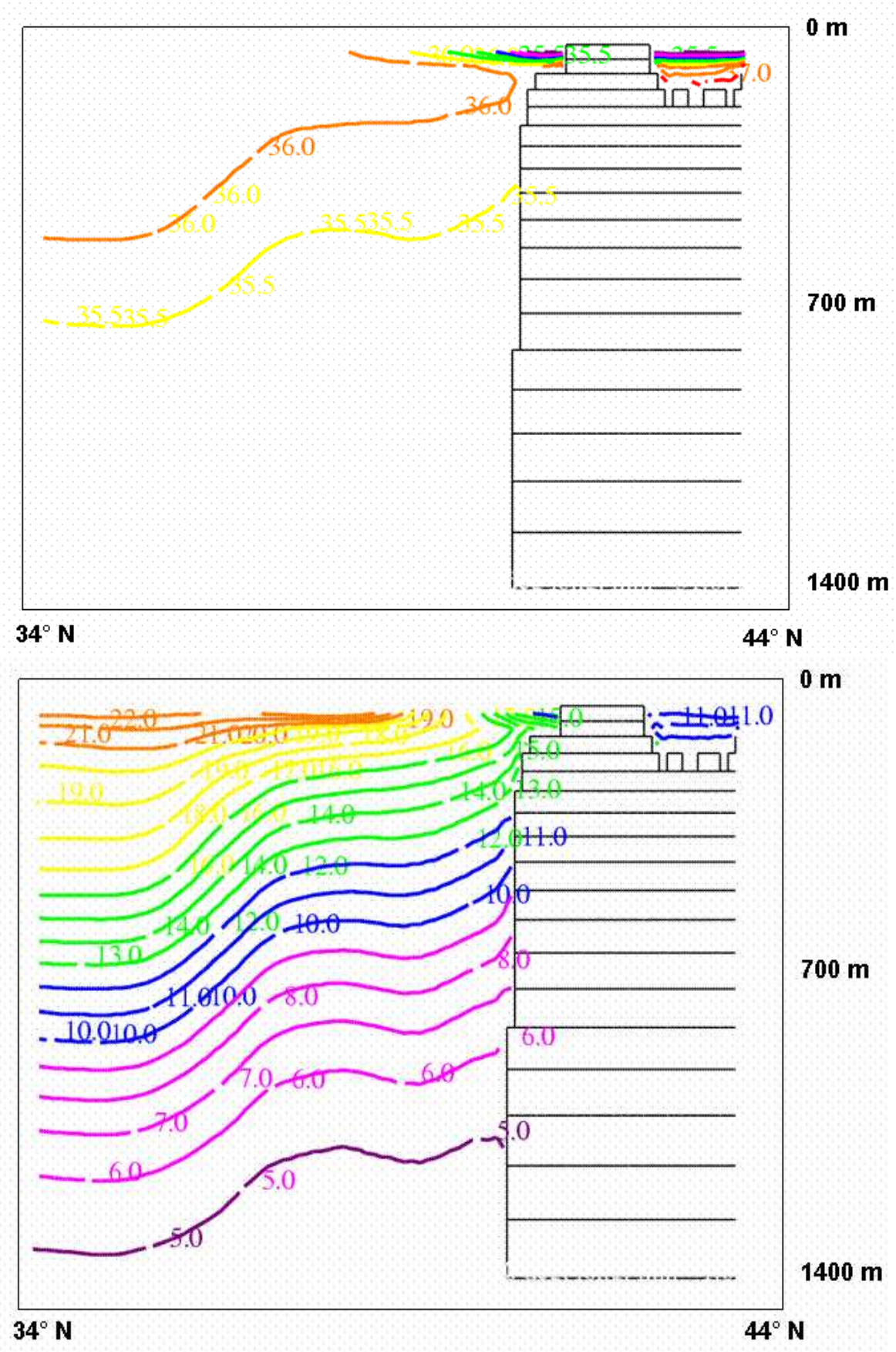

Fig. 6. Vertical/latitudinal cross-sections at 70° W of time-averaged salinity (top) and temperature (bottom) during years 66-75.

Figure 4 shows time mean surface pressure with superposed 700 m depth time averaged velocity vectors during years $1-5$ and years $66-75$. Apparently, the DCS indicated by the deep velocity vectors during years $66-75$, but missing during years $1-5$, plays a big role in the observed mean GS path.

Figures 5 and 6 shows vertical/latitudinal cross-sections at 70° W of temperature averaged during years $1-5$ and years $66-75$ respectively. There is clearly a strong flattening of isopycnal surfaces (well approximated by isotherms) between the DCS and GS core (38° N to 41° N) during the latter years (Figure 6), as in observations (Figure 3). Also during the latter years, there is a strong deepwater GS jet and front outcropping, as in observations.

It follows that model intercomparisons of the GS region before 10 years of simulation, such as done under DAMEE, are of limited value, especially when overly diffused, highly unstable (baroclinically) Levitus climatology is a basis for model comparison, even for time averaged model results, as will be seen below.

The DCS extends to more than 2000 m depth in model results (Figure 7). After turning sharply counterclockwise near CH most of the DCS current travels eastward to well off-shore, before turning southward, crossing under the GS and turning back toward the coast. Transient eddies are significant throughout the depth, and dominate in the deeper levels where the mean flow is smaller. Well converged time average isobars in Figure 7 show significant time mean eddies also occur at these depths. The deep eddies in Figure 7 are graphically enhanced by the small 1 cm (hydrostatic head pressure units) contour interval surface height used to show details of the $O(10)$ cm signal amplitude.

Figures 4-6 show the dramatic effect of the DCS on the GS and the major flattening of isopycnal surfaces that occurs after the DCS dense water reaches the Grand Banks shelfbreak region. Dietrich et al. (2004a) find that a realistically narrower western Labrador Sea shelfbreak significantly intensifies the DCS, resulting in even more strongly flattened isopycnals than seen in Figure 6, more like Yashayaev climatology (Figure 3). Higher model resolution may further intensify the DCS, but is not addressed.

The explanation of the interesting strong GS/DCS interaction indicated by Figures 4-6 is as follows. The Levitus climatology used to initialize the model is unrealistically baroclinic between the observed GS mean location and the Grand Banks shelfbreak, due to smoothing of the climatological data. The resulting baroclinic eddies transport potential density southward (mainly by northward heat transport) and flatten potential density contours in the deep offshore water, leading to strong isopycnal slopes in the shelfbreak region and much weaker slopes along the observed mean GS axis. Thus, there is a north-

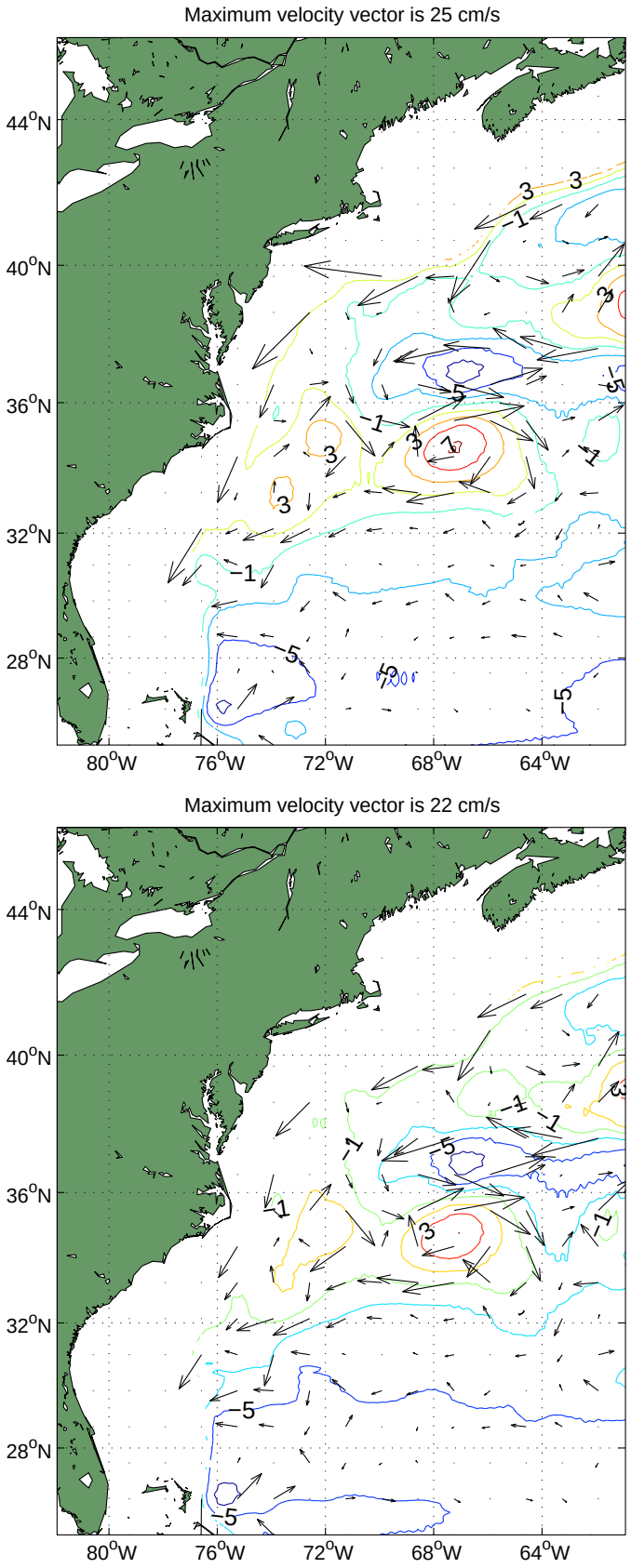

Fig. 7. Time mean pressure in the 1/6° resolution western domain during years $66-75$ at levels 1474 m (top) and 2020 m (bottom).

ward displacement of the GS front to the Grand Banks shelfbreak during the first few model years and a corresponding wrong GS path. Only after full establishment of the DCS along the Grand Banks shelfbreak, which takes ~ 10 model years to occur, does the front move southward to its observed location. This is the time scale required for the densest DCS water formed in the GIN Sea to reach the Grand Banks.

Thus, the DCS water plays a major material role in model GS separation. In a limited area model having specified DCS inflow, Thompson and Schmitz (1989) came to a similar conclusion. The role is analogous to the inner wall of rotating annulus experiments, except the cold water source is by advection of the dense DCS water rather than by conduction at the inner wall. The GS, in turn, plays a role analogous to the outer wall of the rotating annulus experiments. Amplitude vacillation in those experiments is accompanied by flattening of interior isotherms due to baroclinic instability (Pfeffer et al., 1974), which by its very nature results in such flattening. This also characterizes the atmospheric index cycle.

3.2 Other Significant Results

The northern recirculation gyre between the GS and the Grand Banks shelfbreak at depth > 1000 m (Figure 7) entrains and recirculates some of the DCS water. Figure 8 (top) shows its far north source, the East Greenland Current, flowing over the Denmark Strait, which preconditions even deeper water formation in the Labrador Sea. On the east side of the Denmark Strait, a fragment of the North Atlantic Gyre flows into the GIN Sea as observed. Notably, such two-way flow separated by a strong front occurs in spite of the coarse $1/2^\circ$ resolution used in the eastern domain of the present model. The sill overflow quickly becomes a quasi-balanced bottom density current, as the Coriolis terms quickly arrest any initial downslope flow (away from shore) to give a quasi-balanced along-isobath flow with deep water and lower pressure to the left (looking downstream); a slow, frictionally induced cross-isobath (away from shore) flow toward deeper water occurs in the bottom boundary layer (not shown).

Figure 9 shows the time mean rms velocity deviation from the time mean velocity at 700m depth in the Denmark Strait region, where dense sill level water spills "over the dam (sill)" into a bottom density current. The vortex stretching, as the potential energy is released, results in turbulent mixing of the East Greenland Current (Arctic Ocean source) water with the North Atlantic Gyre water. The saddle point structure of the time average surface height (Figure 8 (bottom)) reflects the sill bathymetry, and also shows the mean watermass paths leading to turbulent interaction. Thus, Figures 8-9

indicate inertial, turbulent interaction between the East Greenland Current and North Atlantic Gyre south of the Denmark Strait, even with the relatively coarse 1/2° resolution in this region. The sill overflow is an important part of the thermohaline circulation, and the associated locally strong mixing is important to watermass dynamics.

While some of the DCS upwells on the north side of the GS separation point, some of it continues southward; some of the southward branch upwells on along the shelfbreak between CH and the Bahamas. In Figure 4, the nearly tangential intersection of the negative contours with the coast reflects a top layer source of upwelled DCS water on the west side of the Florida Strait. The cool coastal temperatures in both Yashayaev climatology and model results in this region reflect this upwelling. Horizontal advection by the Florida Current from the south that warms the coastal region is balanced by vertical advection and mixing. This indirect (potential energy increases) secondary vertical circulation includes offshore downwelling as well as nearshore upwelling. It is forced by a combination of bottom drag and entrainment of coastal water into the strong GS current. It thus intensifies the GS front, thereby affecting development of eddies through baroclinic instability, especially after GS separation. In this narrow coastal region, the upwelled undercurrent water is entrained into the Florida Current from the south; this is a region of significant watermass mixing. Unlike the wind forced coastal jet of the California Current system (Haney et al., 2001), local wind effects may be secondary in such an energetic current system. Even the nearshore part of the coastal current, which is the upwelled coastal water indicated by the negative contours in Figure 4, separates almost completely at CH and forms the north wall of the separated GS (located between the green and light blue contour). As noted above, this does not occur as a linear response to the HR winds used in this study.

Figure 10 (online only) shows a sequence of the surface currents during model year 70. A major cold core eddy (often called ring) pinches off the southern tip of a southward GS meander around day 85; around day 100, a warm core pinches off a northward meander. Later, another warm core develops as a result of GS interaction with the New England Seamount Chain: there is a deep northward secondary flow generated by blocking of the deep GS flow, which also steers the northern GS surface current fringe northward into a developing warm core ring, as discussed by Hurlburt and Thompson (1984); this GS bifurcation is (near 64° west) a prevailing feature in model results, as indicated by Figure 4. The GS straightens out to its observed mean path after these two major eddy pinchoffs. These results are consistent with observations of transient small-scale features in and around the GS.

Several times per year, buoyant warm-core eddies pinch off northward meanders of the GS and drift westward and southwestward back through the Middle

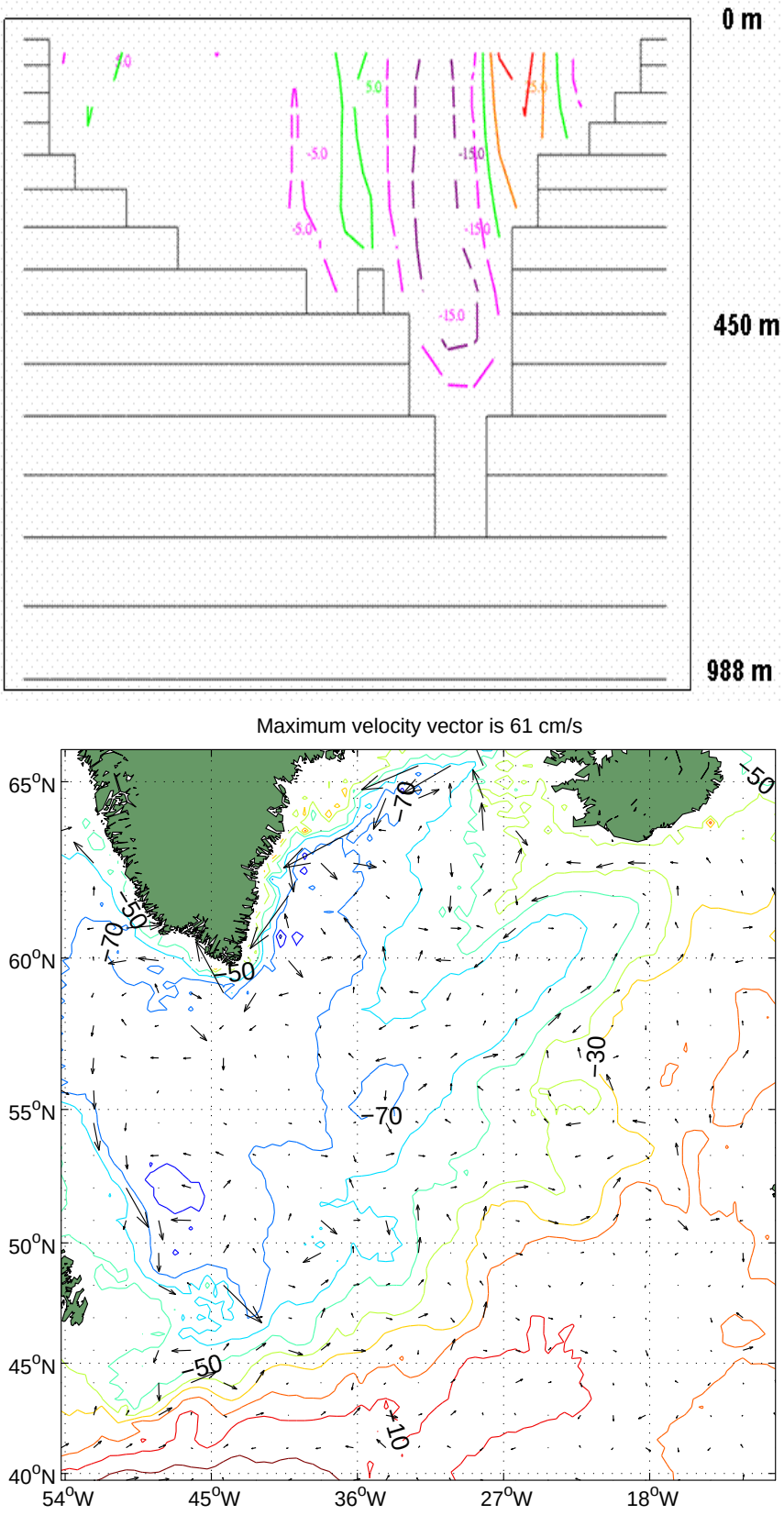

Fig. 8. Vertical/longitudinal cross-section of time mean latitudinal velocity across Denmark Strait (at 65.8° N) in the coarse 1/2° resolution model eastern domain (top); Time mean surface height in the Denmark Strait region (bottom).

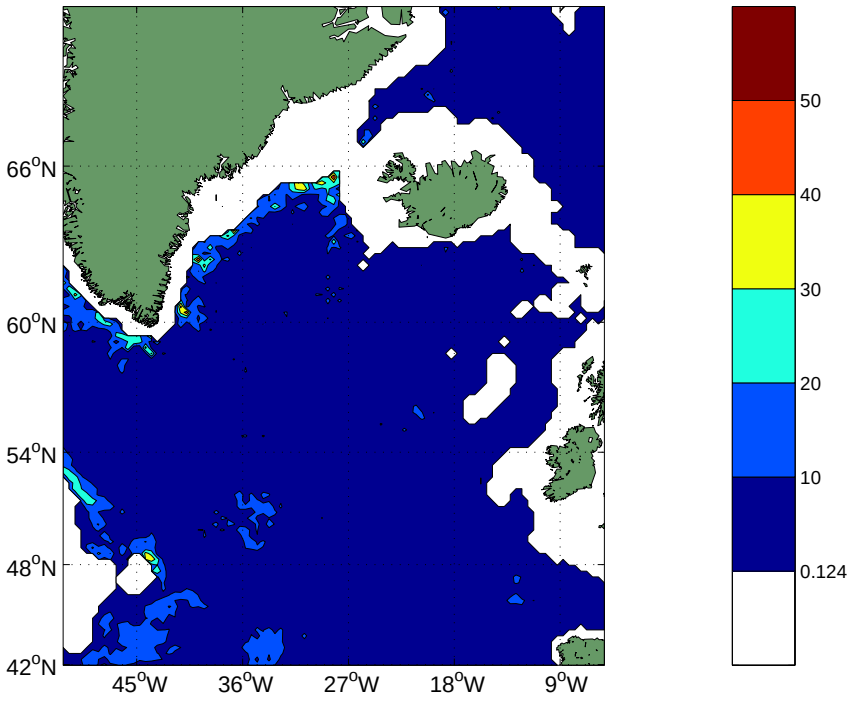

Fig. 9. Time mean rms velocity (cm/s) deviation from the time mean velocity at 700 m depth in the Denmark Strait region.

Atlantic Bight, as also seen in Figure 10. Bowman and Duedall (1975) note that, in nature, they become embedded in the Middle Atlantic Bight shelfslope current and ultimately entrain back into the GS near CH. However, the volume of slope water entrained, including its eddies, is only a fraction of the total $O(100$ Sv) GS transport. Full separation of the warm GS water occurs at Cape Hatteras, including a small volume of much cooler DCS water upwelled along the shelfbreak between the Florida Strait and the Middle Atlantic Bight.

Also in the Figure 10 sequence, the Gulf of Mexico Loop Current penetrates northward and pinches off a major warm core eddy; the Dry Tortuga cyclone (near the southwest coast of Florida) plays a significant role, as do other cyclonic frontal eddies that originate along the Yucatan shelfbreak, some of which merge into the Dry Tortuga eddy when the Loop Current is well extended into the Gulf of Mexico. Some frontal cyclones also pass through the Florida Strait. Before the major warm core eddy pinchoff, the Loop Current takes the shape of a square with rounded corners due to frontal eddy effects. The Loop Current takes a right angle turn into the Florida Strait after eddy shedding. Westward propagating anticyclones prevail in the Caribbean Sea, and there is a semipermanent cyclonic recirculation in the southwestern Caribbean Sea corner. These details are consistent with observations and earlier modeling results (e.g., Dietrich et al., 1997).

Figure 11 shows rms sea surface height anomaly derived from model results. In general, the rms value is $30 - 45$ cm along the separated GS axis all the

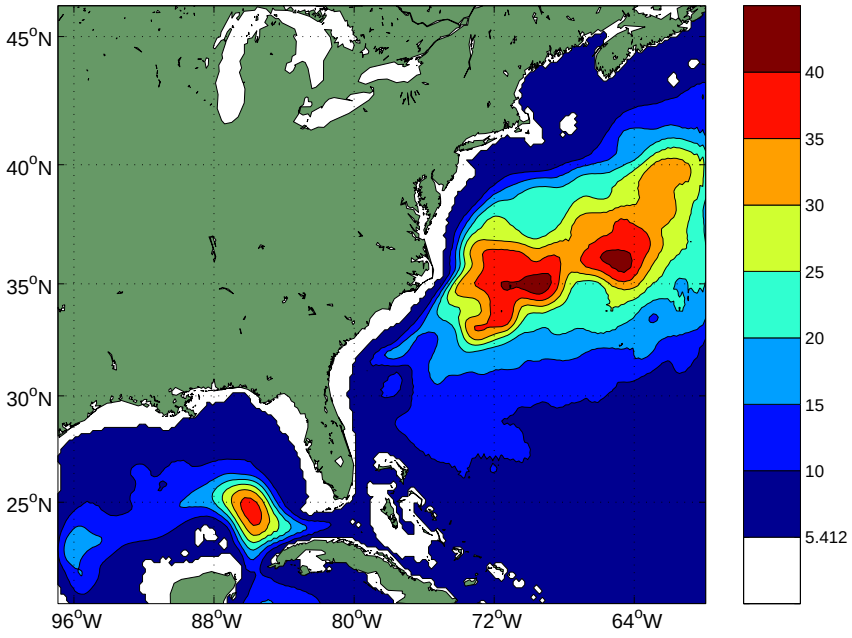

Fig. 11. Root mean square deviation of surface height (cm) from years $66-75$ time mean in western $1/6^\circ$ resolution domain.

way to the New England Seamount region near the eastern boundary of the $1/6^\circ$ resolution grid. Thus, vigorous transient eddies populate the modeled GS region with root-mean-square surface height anomaly amplitudes comparable to those in nature (DYNAMO, 1997 Figure 8.6). The rms anomaly in the Gulf of Mexico region is also close to the observed, as in earlier Gulf of Mexico studies with DieCAST (Dietrich, 1997; Dietrich et al., 1997). The rms value in the coarse resolution domain east of 60° W (not shown) is smaller, but there is a local maximum, 20 cm, along the shelfbreak at the south edge of the Flemish Cap; coupling to low resolution coarse grid domain may cause reduced rms values near the eastern boundary in the fine grid domain.

Although evidence for the creation of 18° mode water is not seen in Figure 6, it is thought that this water is produced episodically (by winter storm events) south of the GS in the Sargasso Sea. (It is unlikely that baroclinically unstable eddies energized by the dense deep western undercurrent systematically transfer only 18° water southward from the GS front.) Climatological surface temperatures do not get this low south of the GS. It is thought that winter storm events create bursts of convection followed by quick recovery to normal climate conditions near the surface, which are then stable. The present simulation has no such storm events in the model forcing, but gradual surface mean cooling keeps the surface layer weakly unstable in the mean during winter.

Using slightly less overall resolution, the present results, calculated on a modern PC, are more realistic than the recent state-of-the-art (Chao et al., 1996). Realistic HR winds, unlike the winds used by Chao et al., do not *force* separa-

tion at CH (Townsend et al., 2000). The mean path of the model GS is close to the observed mean path, starting with a realistic trajectory from the observed separation point. Further downstream, the separated upwelled coastal water bifurcates from the GS core, similar to the two-branch separated Gulf Stream in the linear response to HR winds noted by Townsend et al. (2000). However, this bifurcation is also influenced by interaction with the New England Seamount Chain, as indicated by Figure 10.

3.3 Dispersion, Diffusion and Dissipation Effects

In a diffusivity and viscosity sensitivity study, Dietrich et al. (2004a) show that: in order to get realistic GS separation at CH, the DCS must have sufficient intensity in the New England shelfbreak region to not be blocked by the energetic GS; and the thin, narrow DCS, having long material propagation time from its northern seas and Arctic Ocean source regions, is especially sensitive to these explicit dissipation parameters. The present results further support that finding by showing the details of the early transient in a model having weaker DCS formation due to a more strongly truncated western Labrador Sea than specified by Dietrich et al. (2004a); during the O(10) years early transient, before the weakened DCS forms and penetrates to the CH region, the model GS substantially overshoots CH, but afterward, during the remaining 65 years of the present simulation, the GS separation is much more realistic. Intense synoptic forcing events not included in these studies may strengthen the DCS and reduce its penetration time, but realistic GS separation clearly requires DCS penetration to the CH region.

Thus, getting GS separation requires low numerical dispersion and low numerical and explicit diffusion and viscosity (i.e., low total dissipation). As noted by Sanderson and Brassington (1998): first- and third- order-accurate upwind treatments have inherent numerical dissipation effects; second-order-accurate advection treatment has no inherent dissipation, but has significant numerical dispersion and small-scale numerical overshoots that may occur due to this numerical dispersion (Roache, 1998) unless one includes sufficient explicit diffusion and viscosity, or applies higher order filters that may have less physical basis. Although less explicit diffusion and viscosity may be required in quasi-steady flows (Dietrich et al., 2004a), significant numerical dispersion may still occur with poorly resolved DCS system and its long advection time scales.

An alternate approach having much reduced numerical dispersion is to use fourth-order-accurate advection (Dietrich, 1997), as done here. It thus requires even less explicit diffusion and viscosity to avoid overshoots. This, together with having no dispersion associated with interpolations required for Coriolis term evaluation on the popular Arakawa "C" grid, due to our using a semi-

collocated Arakawa "A" grid control volume framework, allows preservation of a sufficiently intense DCS even in the 1/2 deg resolution eastern domain to get realistic GS separation. This successful DCS maintenance, which includes strong density currents, is due to having less numerical dispersion and dissipation than the approach used by Beckmann and Doscher (1997) in which significant density current dilution occurs due to numerical dispersion and dissipation in idealized test problems. Results from our approach, applied to those idealized test problems, are shown by Dietrich et al. (2004c).

Density current modeling may be further improved by using a thin-shell bottom boundary layer submodel, as Beckmann and Doscher (1997) and Dietrich et al. (1987) suggest, combined with the IBM approach (Tseng and Ferziger, 2003).

4 Other Mechanisms Relating to the Model Results

4.1 Baroclinic Instability Indicated by Observations and Model Results

The wedge shaped region between the separated Gulf Stream and the continental shelf slope is filled with eddies, including striking warm core eddies that pinch off the northern tips of Gulf Stream meanders (Figure 10). The flattened isopycnals in this region's interior, in both climatology and time mean model results (Figures 3 and 6), suggests that the nonlinear eddy system is fueled at least partly by regional potential energy release because, by their very nature and in contrast to diffusive mixing, such potential energy releasing eddies act to *reduce* isopycnal slopes in the region's interior; the larger slopes at the region's boundaries are maintained by open boundary transports from outside the wedge shaped region. This is analogous to the nonlinear wave regime of the rotating annulus experiments, whose interior isotherms have significantly less slope than in more dissipative wave and axisymmetric regimes, while the larger slopes at the boundaries are maintained by conduction at the annular walls (Pfeffer et al., 1974). The characteristically flat nature of the time mean interior isopycnals and the strength of the eddies suggests that dissipation is small, and that little potential energy release is needed to maintain the eddy energy. Based on these observations and model results, we suggest that climatologically important, eddy available potential energy generating, cross-mean-isopycnal potential density transports are small, but concentrated near the wedge edges as a result of frontal eddies. The resulting potential energy release fuels the eddy field, which disperses the energy away from its frontal source regions. To simulate such climatologically important behavior, models must have low dissipation.

Dengg at al. (1996) discuss mechanisms that may play a significant role in GS separation. The present results show that the DCS plays a major role. Dietrich et al. (2004a) show that the low dissipation used in the present study is also very important in order to simulate the observed GS separation and path. Having demonstrated a model giving the observed basic separation and path, we brielfly further discuss separation structure and dynamics, which are of interest to explore by further modeling studies focusing on the CH region.

The upwelled cold water on the shoreward side of the separating GS reflects the lateral convergence of some of the dense DCS water modified in the Labrador Sea. In some models, the DCS does not get around the east end of the Grand Banks with suffient intensity to impact the GS. As shown by Dietrich et al. (2004a) model dissipation and dispersion may cause this loss of DCS intensity. The upwelling enhances the density front, which is primarily subsurface, and thus contributes to the large O(100 Sv) GS transport that is seen in DieCAST results (not shown) and in observations after separation from CH.

Downwelling on the offshore side of the jet increases the buoyancy of the anticyclonic recirculation gyre on the offshore side of the separated jet.

For some features (spatial modes) the recirculation gyre on both sides of the jet are maintained and/or intensified by the fact that features tend to propagate upstream relative to the jet at a rate depending upon the spatial structure of these features and the jet, due to deep and bathymetric Rossby wave effects (Dietrich, 1997). For these modes, the upstream propagation may occur at a rate that nearly balances advection, thus allowing accumulation of warm core water on the south side of the jet and cold core water on the north side, both energized by the separating jet whose energy ultimately comes from the basin scale wind forcing in the well known western boundary current intensification dynamics. These mechanisms are analogous to the nonlinear critical area mechanism sometimes occurring with frontal eddies in the Gulf of Mexico (Dietrich and Ko, 1994; Dietrich et al., 1997).

5 Future Work

Because of the DCS importance, especially to potentially disastrous methane hydrate gasification near the ocean bottom, it would be useful to add a bottom boundary layer submodel, as done relating to risk assessment for burying nuclear waste along the ocean bottom (Dietrich et al., 1987).

It would be interesting to subnest an even finer grid resolution in the vicinity of the GS separation to shed more light on the detailed dynamics of the GS separation, focusing on the vertical circulation in the region of GS separation and how this circulation connects the GS to the DCS.

It would also be interesting to explore whether the GS meanders are such that they take momentum out of the jet or feed the jet. The latter is the antithesis of barotropic instability, as often occurs with finite amplitude effects of baroclinic instability maintaining the mid-latitude jet in the atmosphere (Starr and White, 1951), where baroclinic eddies convert mean potential energy to "eddy available potential energy" (Lorenz, 1955; Lorenz, 1960) and convert the latter to eddy kinetic energy, some of which is lost by nonlinear transports into the mean jet.

6 Concluding Remarks

Results presented herein show that one may simulate GS dynamics and separation from the coast realistically in a marginally eddy-resolving simulation by using a model having: a) low total (physical plus numerical) dissipation; b) fourth-order-accurate advection with its associated low numerical dispersion (Dietrich, 1997; Sanderson and Brassington, 1998); c) further numerical dispersion reduction in the interpolations between grids (Dietrich, 1997); and d) fourth-order-accurate horizontal pressure gradient. Numerical dispersion by the large Coriolis terms is a disadvantage when using the popular Arakawa "c" staggered grid, especially in modeling the thin, narrow DCS with its long natural advection time scale between its source and the Grand Banks shelfbreak; the dense DCS watermass must arrive at the Grand Banks with sufficient intensity to affect the GS separation and ensuing dynamics, as in nature.

Nonlinear dynamics are involved in GS separation, as indicated by modeling studies (Townsend et al., 2000) and theoretical studies (Stern, 1998). It thus seems necessary to resolve the major CH abutment.

However, although bathymetry-induced strongly inertial dynamics may favor separation near CH, our results indicate that it is not sufficient: a robust DCS is also required. Such DCS requires GS separation *somewhere*; nonlinear dynamics choose CH. A robust DCS requires that the DCS water not be dispersed by numerical errors during the $O(10)$ years required for it to travel from its source region to the Grand Banks shelfbreak region.

Overly diffusive models, carefully tuned to Levitus climatology, can closely match this diffused climatology. The present results indicate that this may not be consistent with the strong intense DCS needed to get realistic GS

separation and path. Further, *it is impossible to tune models that require large diffusion for robustness to the observed flattened time averaged non-diffused climatological isopycnals* (Figure 3). This can be done only by a model such as the present DieCAST model configured with low diffusion (Figure 6). The importance of the DCS is enhanced by its interaction with methane hydrates, which may lead to global warming.

Acknowledgments

This work was supported by AcuSea, Inc.; Mississippi State University (contract No. N00014-00-1-0886); and the Naval Postgraduate School (ONR contract no. N0001401WR20092). We gratefully acknowledge Igor Yashayaev, Greg Lukeman and Dan Wright for providing the new Yashayaev climatology and related discussions, and Harley Hurlburt for other helpful discussions.

References

Bacon, S., G. Reverdin, I.G. Rigor and H.M. Smith, 2002. A freshwater jet on the East Greenland shelf. 2002 Ocean Sciences Meeting.

Beckmann, A. and B. Doscher, 1997. A method for improved representation of dense water spreading over topography in geopotential-coordinate models. J. Phys. Oceanogr., 27, 581-591.

Bowman, M.J., and I.W. Duedall, 1975. Gulf Stream meander in the vicinity of the New York Bight. Gulfstream, 1 (2), 6-7, 1975. NOAA, Washington, D.C.

Chao, Y., A. Gangopadhyay, F.O. Bryan and W.R. Holland, 1996. Modeling the Gulf Stream system: How far from reality?. Geophys. Res. Lett., 23, 3155-3158.

Chapman, D.C. and P.C. Beardsley, 1989. On the Origin of Shelf Water in the Middle Atlantic Bight. J. Phys. Oceanogr., 19, pp. 384-391.

Cushman-Roisin, B., K.A. Korotenko and D.E. Dietrich, 2003. Mesoscale Dynamics in the northern and middle Adriatic Sea. EGS-AGU-EUG Joint Assembly, Nice, France, April 2003

Dengg, J., A. Beckmann and R. Gerdes, 1996. The Gulf Stream separation problem. In: Krauss, W. (Ed.), The warmwatersphere of the North Atlantic Ocean. Gebr. Borntraeger, Berlin, 253-290.

Dietrich, D.E., A. Mehra, R.L. Haney, M.J. Bowman, and Y.H. Tseng, 2004a. Dissipation Effects in Modeling the North Atlantic Ocean Geophys. Res. Lett. (in press).

Dietrich, D.E., R.L. Haney, V. Fernandez, S. Josey and J. Tintore, 2004b. Air-sea fluxes based on observed annual cycle surface climatology and ocean

model internal dynamics: a precise, non-damping, zero-phase-lag approach applied to the Mediterranean Sea. J. Mar. Systems (in press).

Dietrich, D.E., Y.H. Tseng, A. Mehra, R.L. Haney and S. Piacsek, 2004c. Modeling of dense deep currents along the ocean bottom. To be submitted.

Dietrich, D.E., 2002. Duo-resolution North Atlantic Ocean/Gulf of Mexico model. 2002 Ocean Sciences Meeting.

Dietrich, D.E. and A. Mehra, 1998. Sensitivity Studies in the Santa Barbara Channel using the DieCAST Ocean Model. Proceedings of the Santa Barbara Channel Quality Review Board Meeting, San Diego, February, 1998.

Dietrich, D.E., 1997. Application of a Modified "a" Grid Ocean Model Having Reduced Numerical Dispersion to the Gulf of Mexico Circulation. Dynamics of Atmospheres and Oceans, 27, 201-217.

Dietrich, D.E., C.A. Lin, A. Mestas-Nunez and D.-S. Ko, 1997. A High Resolution Numerical Study of Gulf of Mexico Fronts and Eddies. Meteorol. Atmos. Phys., 64, 187-201.

Dietrich, D.E., M.J. Bowman, C.A. Lin, and A. Mestas-Nunez, 1996. Numerical Studies of Small Island Wakes. Geophys. Astrophys. Fluid Dynamics, 83, 195-231.

Dietrich, D.E. and D-S. Ko, 1994. A Semi-Collocated Ocean Model Based on the SOMS Approach. Int. J. Numer. Methods in Fluids, 19, 1103-1113.

Dietrich, D.E., M.G. Marietta and P.J. Roache, 1987. An ocean modeling system with turbulent boundary-layers and topography. Part I: Numerical Description. Int. J. Numer. Methods Fluids, 7, 833-855.

DAMEE-NAB, 2000. Data assimilation and model evaluation experiment - North Atlantic Basin. Dyn. Atmos. Oceans., 32, special DAMEE-NAB issue.

DYNAMO, 1997. Dynamics of North Atlantic Models. Simulation and assimilation with high resolution models. Institure fur Meereskunde an der Univsrsitat Kiel, 334 pp.

Fernandez, V., D.E. Dietrich, R.L. Haney and J. Tintore, 2003. Mesoscale, Seasonal and Interannual Variability in the Mediterranean Sea using the DieCAST Ocean Model. *Submitted to J. Marine Systems (in revision).*

Haidvogel, D.B., H.G. Arango, K. Hedstrom, A. Beckmann, P. Malonotte-Rizzoli and A.F. Shchepetkin, 2000. Model evaluation experiments in the North Atlantic Basin: simulations in nonlinear terrain-following coordinates. Dyn. Atmos. Oceans., 32, 239-281.

Haney, R.L., R.A. Hale and D.E. Dietrich, 2001. Offshore propagation of eddy kinetic energy in the California Current. JGR-Oceans, 106, C6, 11,709-11,717.

Hellerman, S. and M. Rosenstein, 1983. Normal monthly wind stress over the world ocean with error estimates. J. Phys. Oceanogr., 13, 1093- 1104.

Hurlburt, H.E. and P.J. Hogan, 2000. Impact of 1/8 deg to 1/64 deg resolution on Gulf Stream model-data comparisons in basin-scale subtropical Atlantic Ocean models. Dyn. Atmos. Oceans., 32, pp. 283- 329.

Hurlburt, H.E. and J.D. Thompson, 1984. Preliminary results from a numerical study of the New England Seamount chain influence on the Gulf Stream.

Proc. of the Workshop on Predictability of Fluid Motions, Amer. Inst. Phys. G. Hollaway, Ed.

Hurlburt, H.E. and J.D. Thompson, 1980. A numerical study of Loop Current intrusions and eddy shedding. J. Phys. Oceanogr., 10, 1611-1651.

IPCC, 2001: Climate Change 2001: The Scientific basis; Cambridge University Press. 874 pp.

Joos, F, G-K Plattner, T. F. Stocker, A Kortzinger and D.W.R. Wallace, 2003. Trends in marine dissolved oxygen: Implications for ocean circulation changes and the carbon budget. EOS, Transaction of American Geophysical Union. Vol. 84, No. 21, 197 - 201.

Katz, M.E., D.K. Pak, G.R. Dickens and K.G. Miller, 1999. The source and fate of massive carbon input during the latest paleocene thermal maximum. Science. Vol. 286, No. 5444, 1531 - 1533.

Kennett, J.P., K.G. Cannariato, I.L. Hy, and R.J. Behl, 2000. Carbon isotopic evidence for methane hydrate instability during Quaternary Interstadials. Science. 288, 128 - 133.

Killworth, P.D., D.A. Smeed and A.J.G. Nurser, 2000. The effects on ocean models of relaxation toward observations at the surface. J. Phys. Oceanogr., 30, 160-174.

Lai, C-C. A., 2003. Personal communication.

Lorenz, E.N., 1955. Available potential energy and the maintenance of the general circulation. Tellus, 7, 157-167.

Lorenz, E.N., 1960. Generation of available potential energy and the intensity of the general circulation. Dynamics of Climate. R.L.Pfeffer, Ed., New York, Pergamon Press, 86-92.

Pfeffer, R.L., G. Buzyna and W.W. Fowlis, 1974. Synoptic features and energetics of wave-amplitude vacillation in a rotating, differentially heated fluid. J. Atmos. Sci., 31, pp. 622-645.

Rahmstorf, S. and R.B. Alley, 2002. Stochastic resonance in glacial climate. EOS, 19 March, 2002 (lead article).

Roache, P.J., 1998. Fundamentals of Computational Fluid Dynamics. Hermosa Publishers.

Rossby, T. and J. Nilsson, 2003. Current switching as the cause of rapid warming at the end of the last Glacial Maximum and Younger Dryas. Geophys. Res. Lett., 30, 1051-1054.

Sanderson, B.G. and G. Brassington, 1998. Accuracy in the context of a control-volume model. Atmosphere-Ocean, 36, 355-384.

Staneva, J.V., D.E. Dietrich, E.V. Stanev and M.J. Bowman, 2001. Rim Current and Coastal Eddy Mechanisms in an Eddy-Resolving Black Sea General Circulation Model. J. Marine Systems, special issue on the Black Sea, 31, pp. 137-157.

Starr, V.P. and R.M. White, 1951. A hemispherical study of the atmospheric angular-momentum balance. Q. J. Roy. Meteor. Soc., 77, 215-225.

Stern, M.E., 1998. Separation of a density current from the bottom of a continental slope. J. Phys. Oceanogr., 28, 2040-2049.

Thompson, J.D. and W.J. Schmitz, 1989. A limited-area model of the Gulf Stream: design, initial experiments and model-data intercomparison. J. Phys. Oceanogr., 19, 791-814.

Townsend, T.L., H.E. Hurlburt and P.J. Hogan, 2000. Modeled Sverdrup flow in the North Atlantic from 11 different wind stress climatologies. Dyn. Atmos. Oceans.,, 32, 373-417.

Tseng, Y.H. and J. Ferziger. A ghost-cell immersed boundary method for flow in complex geometry. J. Comput. Phys., 192, 593-623, 2003.

Velez-Belchi, P., A. Alvarez, P. Colet, J. Tintore and R.L. Haney, 2001. Stochastic Resonance in the Thermohaline Circulation. Geophys. Res. Lett., 28, 2053-2056, 2001.

Yashayaev, I.,2002. Personal communication.
http://www.mar.dfo-mpo.gc.ca/ science/ocean/woce/climatology/naclimatology.htm